

Fatigue-free, superstretchable, transparent, and biocompatible metal electrodes

Chuan Fei Guo^a, Qihan Liu^b, Guohui Wang^{c,d}, Yecheng Wang^b, Zhengzheng Shi^c, Zhigang Suo^b, Ching-Wu Chu^{a,e,1}, and Zhifeng Ren^{a,1}

^aDepartment of Physics and Texas Center for Superconductivity, University of Houston, Houston, TX 77204; ^bSchool of Engineering and Applied Sciences, Kavli Institute for Bionano Science and Technology, Harvard University, Cambridge, MA 02138; ^cDepartment of Translational Imaging, Houston Methodist Research Institute, Houston, TX 77030; ^dDepartment of Internal Medicine, The Affiliated Tumor Hospital of Zhengzhou University, Zhengzhou, Henan 450003, People's Republic of China; and ^eLawrence Berkeley National Laboratory, Berkeley, CA 94720

Contributed by Ching-Wu Chu, August 25, 2015 (sent for review July 29, 2015; reviewed by Hui-Ming Cheng and Hui Wu)

Next-generation flexible electronics require highly stretchable and transparent electrodes. Few electronic conductors are both transparent and stretchable, and even fewer can be cyclically stretched to a large strain without causing fatigue. Fatigue, which is often an issue of strained materials causing failure at low strain levels of cyclic loading, is detrimental to materials under repeated loads in practical applications. Here we show that optimizing topology and/or tuning adhesion of metal nanomeshes can significantly improve stretchability and eliminate strain fatigue. The ligaments in an Au nanomesh on a slippery substrate can locally shift to relax stress upon stretching and return to the original configuration when stress is removed. The Au nanomesh keeps a low sheet resistance and high transparency, comparable to those of strain-free indium tin oxide films, when the nanomesh is stretched to a strain of 300%, or shows no fatigue after 50,000 stretches to a strain up to 150%. Moreover, the Au nanomesh is biocompatible and penetrable to biomacromolecules in fluid. The superstretchable transparent conductors are highly desirable for stretchable photoelectronics, electronic skins, and implantable electronics.

fatigue-free | adhesion | biocompatibility | topology | stretchability

Flexible transparent electrodes are crucial to the emerging fields of flexible solar cells (1, 2), flexible electronics (3–5), electronic skins (e-skins) (6), and implantable electronics (7, 8). Among the several modes of flexibility, including bending, folding, twisting, and stretching, stretching generates the largest strain and therefore is the most demanding (9). What is even more challenging is to make transparent electrodes fatigue-free under cyclic stretches. Fatigue often happens during strain cycling, even if the strain level is relatively low. It determines the real loading that can be applied to a material in practical applications. However, metallic materials often exhibit high cycle fatigue (10), and fatigue has been a deadly disease for metals.

Several types of transparent conductors, including graphene sheets, carbon nanotube (CNT) films, metal nanowire (NW) networks, composites based on Ag NWs, metal meshes, and ultrathin metal films have been found to be stretchable (1, 3, 6, 11–18). However, sheet resistance (R_{sh}) of existing stretchable transparent electrodes often sharply increases when highly stretched, or repeatedly stretched to relatively small strains for thousands of cycles. Graphene can be stretched one time to 30%, or cyclically stretched to 6% for a few times (11). Metal meshes made of straight lines and ultrathin metal films are also stretchable, but typically they cannot be stretched to more than 100% (16, 17). The Bao group has shown that CNT network film with a serpentine morphology can be stretched one time to 170% before failure, or repeatedly stretched to 25% for 12,500 cycles with a modest increase of resistance (6). Here we show that optimizing topology of a Au nanomesh can significantly improve the stretchability, revealing an R_{sh} of $\sim 28 \Omega/\square$ and a transmittance (T) $\sim 90\%$ when stretched to 300%. Moreover, by tuning the adhesion between the Au nanomesh and the underlying substrate, the conductor exhibits high fatigue resistance:

The resistance does not increase and the morphology has little change after 50,000 cycles of stretching to a large strain of 150%. We ascribe the fatigue-free nature to two reasons. First, the ligaments in the Au nanomesh on a slippery substrate can locally shift and reorient to relax stress. Second, the Au nanoserpentine are well interconnected, and the nodes play an important role for the metal nanomesh to return to the original shape after stress is removed. The Au nanomesh is also biocompatible, and penetrable to body fluid, allowing biomacromolecules to pass through freely. The large stretchability, high fatigue resistance, and good biocompatibility of the transparent electrode are highly desired for stretchable photoelectronics, e-skins, and implantable electrodes in medical devices.

Experimental Procedures

Fabrication and Characterization of Au Nanomeshes. The fabrication of the Au nanomeshes can be found in ref. 18. We obtained compressed Au nanomeshes by using a prestretched polydimethylsiloxane (PDMS) substrate to adhere free-floating Au nanomesh and drying with compressed airflow, followed by releasing the PDMS substrate slowly. The PDMS substrates (curing agent:base = 1:12, volume ratio) were typically 2–3 mm wide, 5 mm long, and 0.1–0.2 mm thick, with two ends bonded on 3-mm-thick and 10-mm-wide PDMS anchors (curing agent:base = 1:8), on which contact (very thick Au nanowire network with R_{sh} lower than $1 \Omega/\square$ covering the whole anchor) was made. The anchors were clamped and connected to a source meter during stretching. This design does not damage the contact even when the electrode is highly stretched. The adhesion between the Au nanomesh and the underlying PDMS is tuned to three levels: poor (on slippery substrate), medium (on as-cured substrate), and strong (forming a chemical bond). A thin layer of oil (PDMS base) was applied to decrease adhesion, and a monolayer of trimethoxysilylpropanethiol molecules was assembled on oxidized PDMS to form a chemical bond with Au to enhance adhesion. Stretching cycling was performed at a strain rate of $\sim 75\% \cdot s^{-1}$, and one-time stretching

Significance

Fatigue is a deadly disease for metals. Fatigue often happens under cyclic loading even if the strain level is low. However, a stretchable transparent electrode, which can be made of metal and is a key element in stretchable electronics, needs high stability at large strains. Here we show that Au nanomesh on a slippery substrate is fatigue-free when cyclically stretched to large strains (>100%). Moreover, cells can grow on the Au nanomesh. A metal mesh that conducts electricity, is biocompatible, and is completely free of fatigue will be an ideal electrode not only for flexible electronics, but also for implantable electronics.

Author contributions: C.F.G. and Z.R. designed research; C.F.G. and G.W. performed research; C.F.G., Q.L., Y.W., Z. Shi, and Z. Suo analyzed data; and C.F.G., C.-W.C., and Z.R. wrote the paper.

Reviewers: H.-M.C., Institute of Metal Research, Chinese Academy of Sciences; and H.W., Tsinghua University.

The authors declare no conflict of interest.

¹To whom correspondence may be addressed. Email: cwchu@uh.edu or zren@uh.edu.

This article contains supporting information online at www.pnas.org/lookup/suppl/doi:10.1073/pnas.1516873112/-DCSupplemental.

and bending cycling were performed at a strain rate of $\sim 25\% \cdot s^{-1}$. Transmittance was measured using a Hitachi U2001 spectrometer. Scanning electron microscopy (SEM) images were taken using a LEO 1525 scanning electron microscope. Atomic force microscopy images were taken using a D-3100 atomic force microscope from Digital Instruments, Inc.

Cell Culture. Mouse embryonic fibroblast (MEF) cells were derived from mouse embryos at embryonic day E12.5 (MEF 38) and E14.5 (MEF 178) according to the standard procedures (19) and frozen with liquid nitrogen at passage 1 (P1). The MEF cells were thawed and cultured in Dulbecco's modified eagle medium containing 10% FBS and penicillin-streptomycin ($10,000 \text{ U}\cdot\text{mL}^{-1}$). The passage 2 (P2) cells were plated in 96-well plates, with the well bottom covered with an Au nanomesh, or without it, at 7,000 cells per well. On the third day, $10 \mu\text{L}$ of CCK-8 reagent (Cell Counting Kit-8; Dojindo Molecular Technologies, Inc.) was added to each well of the plate, and the cells were incubated for 2 h and measured for absorbance at 450 nm using a microplate reader, and calculated for the relative cell growth rate. Additionally, cells were seeded on a six-well plate at 5×10^5 cells per well with the wells covered with or without Au nanomeshes and cultured for 6 or 13 d for morphological observation. The P values were calculated from four independent experiments ($n = 4$, Student t test).

Penetrability. Seven milliliters of water and 3 mL fluorescent BSA solution were placed in two wells connected with a 10×10 -mm hole, separated by a Au nanomesh supported on a piece of filter paper. After 50 min of diffusion, 1 mL of solution from the water side was extracted for an absorbance test. A control experiment without an Au nanomesh was also conducted.

Results and Discussion

The Effect of Topology on Stretchability and Transmittance. Many flexible transparent conductors present a mesh configuration. For simplicity, we discuss mesh-like thin structures with a basic unit ($a_0 \times 2b_0$), and line width w , as indicated in the red dashed area) shown in Fig. 1A, which can be stretchable along the b axis. The stretchability of the structure, characterized as the maximum elongation (e_{max}) before failure (or the regime in which the paper

mesh deforms totally elastically) is related to the ratio of a_0/b_0 . From Fig. S1, e_{max} can be expressed as

$$e_{\text{max}} = \frac{b(\epsilon) - w}{b_0} + \frac{\sqrt{w^2 + [a(\epsilon)/2 - w]^2}}{b_0} - 1, \quad [1]$$

where b_0 is the original length of b and $a(\epsilon)$ and $b(\epsilon)$ are strain (ϵ)-dependent a and b , respectively. Fig. 1B plots e_{max} as a function of a_0/b_0 and w/b_0 and it shows that stretchability increases with the increasing of the ratio a_0/b_0 . Our experiments by stretching paper meshes show that as the a_0/b_0 ratio increases from 0.5 to 1.0 to 2.3, e_{max} increases consequently from 12 to 33 to 82% (Fig. 1C–E). From Eq. 1, e_{max} further increases if $a(\epsilon)$ and/or $b(\epsilon)$ increases. It has been proven that serpentines can be elongated, so if we replace the straight lines with serpentines, the mesh can be more stretchable. In Fig. 1F, we replace straight lines b with serpentines and this structure presents a much larger e_{max} of 110% compared with the counterpart with straight lines ($e_{\text{max}} = 82\%$) in Fig. 1E. Although stretching the paper mesh by hand may not provide very accurate values of strain, the measured values of e_{max} provide a good demonstration to reveal the approximate effect of changing a_0/b_0 on stretchability. The result can be extended to other materials including carbon nanotubes and metals in the elastic regime.

Practically, it is difficult to fabricate nanoscale metal structures with a large a_0/b_0 ratio and serpentine nanowires by using conventional nanofabrication methods. The Au nanomesh in this study is fabricated by using a method that we call grain boundary lithography (18). The grain boundary lithography includes depositing an indium film and etching to form a mask layer, followed by bilayer metallization (18, 20). The as-made Au nanomeshes consist of well-interconnected, serpentine Au ligaments (Fig. 2A) with a line width of ~ 70 nm, a thickness of ~ 40 nm, and a mesh size of $\sim 1 \mu\text{m}$, exhibiting a sheet resistance (R_{sh}) of 20–30 Ω/\square and

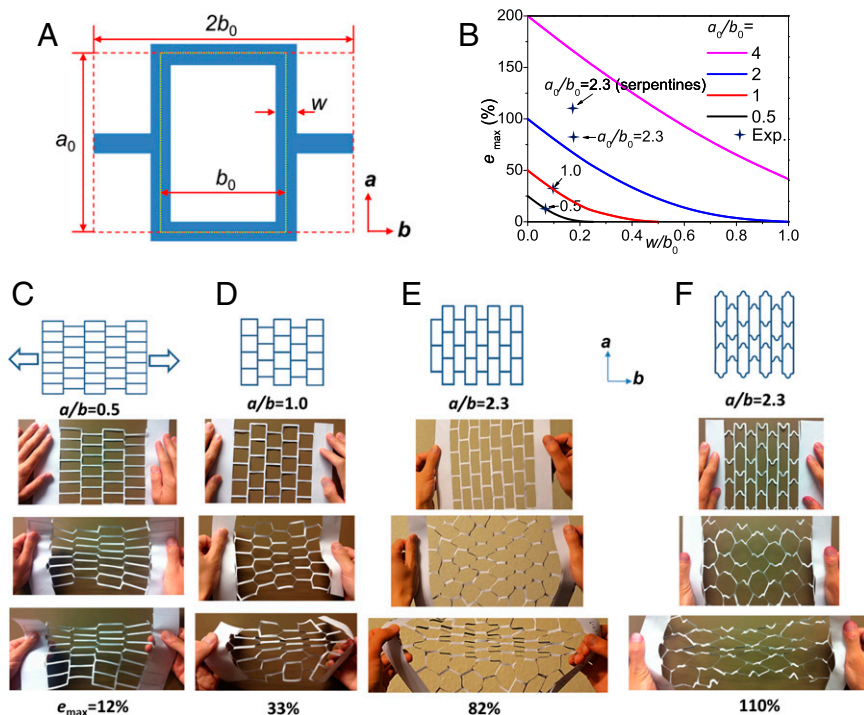


Fig. 1. The effect of topology of networks on stretchability. (A) A basic unit of a stretchable network. (B) e_{max} as a function of w/b_0 and a_0/b_0 . The crosses are extracted from the experimental data of panels C–E. (C–E) By changing the ratio of a_0/b_0 from 0.5 to 1.0 and to 2.3, the corresponding maximum elongation e_{max} changes from 12 to 33% and to 82%, respectively. (F) A network with serpentines and an a_0/b_0 ratio of 2.3 can be stretched to 110%.

a transmittance (T) close to 90%. The Au nanomesh is then transferred to a prestretched PDMS substrate followed by releasing. We could see that the prestretched Au nanomesh (Fig. 2B) exhibits a larger “ a_0/b_0 ratio” and serpentine ligaments, similar to the paper mesh in Fig. 1F, while only lacking ordering.

Fig. 2C shows the change of resistance (R/R_0 , where R is the measured resistance and R_0 is the original resistance before stretching) under stretching for Au nanomeshes with prestrains of 0, 50, 100, and 150%. The resistance of the sample with a 150% prestrain does not increase until stretched to a strain of 120% and only increases 1.6 times ($R_s/R_0 = 2.6$, R_s is the resistance under stretched state) by one-time stretching to a ultralarge strain of 300%; the corresponding resistance after releasing strain (R_r) only increases by 19% compared with the original value. The large stretchability is better than the best reported results of percolating network including CNT films (6), Ag NW network-based composite films (15), metal nanotrough networks (16), and nonprestrained Au nanomeshes (18) (Fig. S2). Our experiments over tens of samples show that the Au nanomesh does not fail until the PDMS substrate breaks.

Although the one-time stretchability is dramatically enhanced with the increasing of prestrain, we show in Fig. 2D that the optical transmittance slightly decreases. The average transmittance in the wavelength range of 400–1,000 nm changes from 89.2%, 85.4%, 82.6%, and 79.7% with a prestrain of 0, 25, 50, 75, and 100%, respectively, as a result of increasing density of Au nanomeshes per area. The result indicates that the prestrained Au nanomeshes lose a few percent of transmittance but gain a huge stretchability. At a highly stretched state of 300% strain, the Au nanomesh exhibits a $T \sim 90\%$ and an $R_{sh} \sim 28 \Omega/\square$ (shown in Fig. 2C), superior to that of any existing highly stretchable and transparent electronic conductors (6, 15, 16), or even ionic conductors at highly stretched state (21).

The Effect of Adhesion on Strain Fatigue. The prestrained Au nanomesh on as-made PDMS is superstretchable; however, strain fatigue happens even when the applied cyclic strain is smaller than the prestrain. In Fig. 2E, resistance of the prestrained (150%) Au nanomesh under stretches to 75% begins to increase after 1,000 cycles from a slightly decreased value and both R_s and R_r exceed R_0

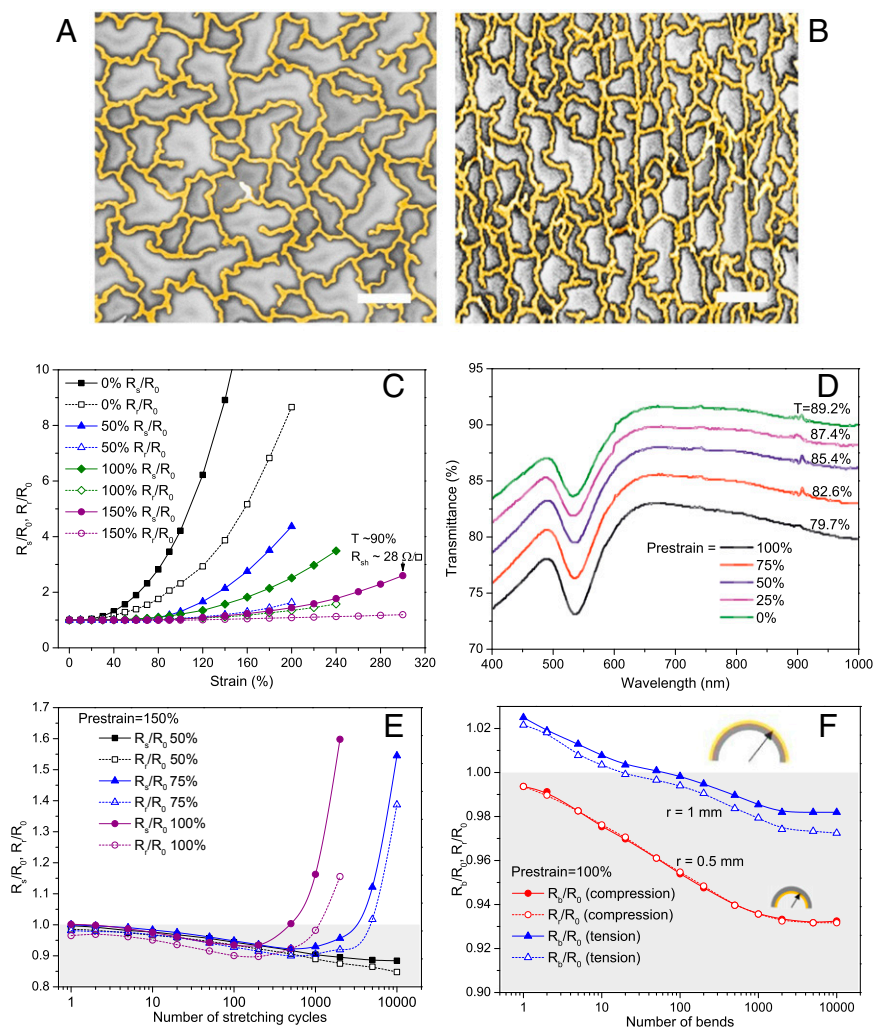


Fig. 2. Stretchability, transmittance, and strain fatigue of prestrained Au nanomeshes on as-cured PDMS. (A and B) SEM images of as-made and prestrained Au nanomeshes on PDMS, respectively. (Scale bars, 1 μm .) (C) R_s/R_0 and R_r/R_0 as a function of strain for Au nanomeshes with different prestrains of 0, 50, 100, and 150%. Both R_s/R_0 and R_r/R_0 for each nanomesh are shown. The sample with a 150% prestrain has a $T \sim 90\%$ and an $R_{sh} \sim 28 \Omega/\square$ when stretched to 300%. (D) Transmittance of an Au nanomesh under different prestrains of 0, 25, 50, 75, and 100%, indicating that T slightly decreases with the increasing of prestrain. (E) Strain cycling of prestrained (150%) Au nanomeshes under tensile strains of 50, 75, and 100%. (F) R_b/R_0 (R_b is the resistance under bending) and R_c/R_0 (R_c is the resistance under compression) by bending up to 10,000 cycles for an Au nanomesh with a 100% prestrain. No fatigue is shown for bending with tension (bending radius $r = 1$ mm) or compression ($r = 0.5$ mm).

after 5,000 cycles; when cycled for 10,000 stretches, R_s increases by $\sim 55\%$. As loaded strain increases to 100%, the resistance increases much faster: R_s begins to exceed R_0 after only 500 stretching cycles, and R_s/R_0 increases by a factor of 60% after only 2,000 cycles. It is interesting that the resistance decreases in the first hundreds of cycles. This is due to deformation-induced cold welding of Au nanowires (22). The cold welding competes with plasticity in the Au nanomesh. When the applied cyclic strain is small, the healing effect from the cold welding can overcome the effect of plastic deformation. We show in Fig. 2E that the Au nanomesh does not exhibit strain fatigue when it is stretched to 50% for 10,000 cycles. Fig. 2F shows that under cyclic bends with a bending radius (r) of 0.5 mm (with a nominal bending strain of $\sim 8\%$) or 1 mm (with a nominal stretching strain of $\sim 4\%$), the resistance of the Au nanomesh with a 100% prestrain does not increase even after 10,000 bending cycles because bending generates much smaller strains.

The fatigue of the Au nanomesh on as-cured PDMS stems from the fact that the plastic component, although a small part of the deformation in the nanomesh, can result in rupture of some Au nanowires. A completely elastic material does not suffer from fatigue, so it is therefore necessary to decrease the stress level. Here we show that the adhesion has a strong effect on the fatigue of the Au nanomesh. For a free-standing mesh structure (no adhesion), large strain is mainly accommodated by the stretching and narrowing of the pores of the mesh (Fig. 3A). Each ligament may rotate and shift in space, but the strain in the ligament is small. The displacement of the ligament depends on the local geometry and is in general nonhomogenous. By contrast, if such a mesh is well bonded onto an elastomeric substrate that imposes a homogenous displacement field, the aforementioned mechanism of rotation and shift is strongly constrained. As a result, we see the mesh broken into isolated islands under modest stretches (Fig. 3B).

We weaken the constraint of the substrate by making the interface between the Au nanomesh and PDMS slippery, and expect the Au nanomesh to achieve superstretchability and high fatigue resistance. Free of fatigue here means that both the structure and the resistance do not change or have little change after many strain cycles. We show that an Au nanomesh with a prestrain of 100% on a slippery substrate keeps the morphology after being stretched to 100% for 54,000 cycles (Fig. 3C and D). The Au nanomesh deforms elastically upon stretching and returns back to the original configuration when strain is released no matter how many cycles are applied. The nodes in the mesh or the well-interconnected nature may play an important role for the structure to recover (23). By contrast, the counterpart on an as-cured substrate (with a stronger adhesion) forms large cracks after being stretched to 100% for only 1,000 cycles (Fig. 3E and F). The Au nanomeshes on slippery substrates also have a relatively stable resistance when stretched. For an Au nanomesh on slippery PDMS with a prestrain of 150%, R_s/R_0 increases by only 29% when stretched to 200% (Fig. 3G). More importantly, the Au nanomesh exhibits only a small change in resistance (Fig. 3H) when cyclically stretched to a strain up to 150% for more than 10,000 cycles. The Au nanomesh with a prestrain of 100% stretched to 100% for 54,000 cycles has an R_s/R_0 of only 1.09; when stretched to a strain of 120% (which is larger than the prestrain), there is still no fatigue after stretching for 32,000 cycles. Here we use the criteria of Sim et al. (24) that fatigue-free means R/R_0 is less than 1.25. The Au nanomesh with a 150% prestrain has an R_s/R_0 of 1.12 after 50,000 cycles of stretches to a large strain of 150%; the corresponding R_{sh} is $\sim 25 \Omega/\square$ and T is $\sim 85\%$ at the stretched state. The fatigue resistance of the Au nanomesh on a slippery substrate is superior to that of any existing stretchable transparent electrodes, among which the most impressive is a CNT film that was free of fatigue after being stretched to 25% for 12,500 cycles. However, this CNT conductor exhibits a

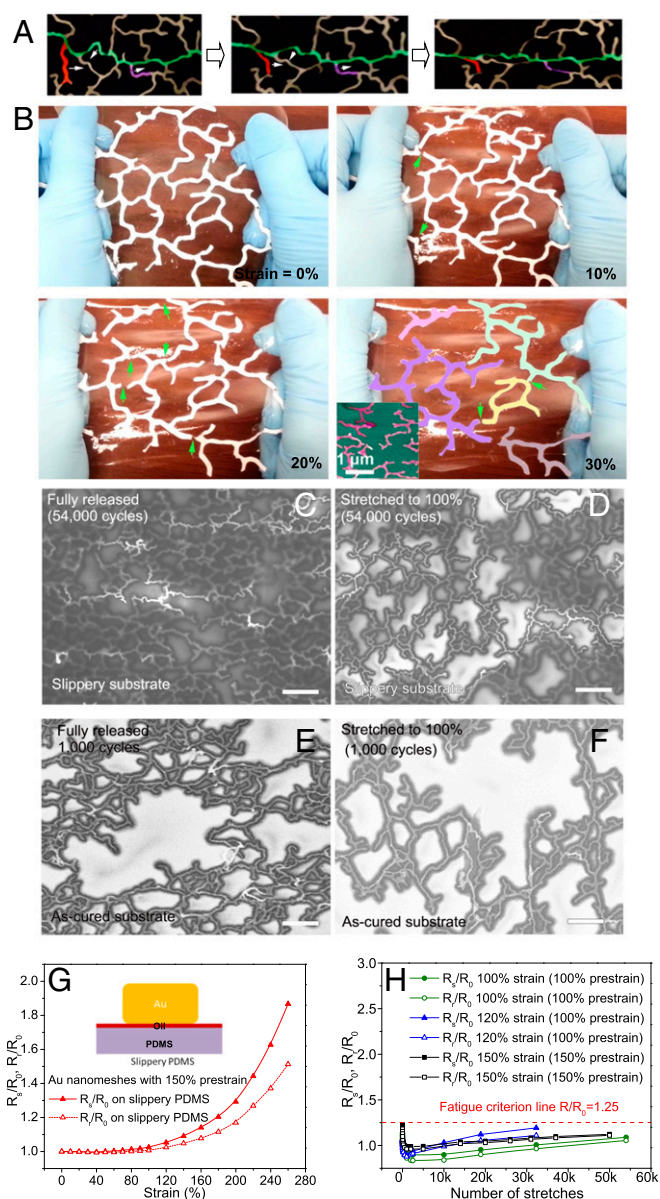


Fig. 3. The effect of adhesion on stretchability and strain fatigue. (A) Deformation of the ligaments in a free-standing paper mesh (which has the same effect as the mesh on a slippery substrate) in a stretch cycle. Ligaments slide and reorient upon deformation (exemplified by the ones in green, red, and purple, for which the intersection angles between them changes) to release stresses. White arrows indicate the directions in which the ligaments shift. (B) Ligaments of a mesh well-bonded on PDMS break locally (indicated by the green arrows) upon stretching. The mesh breaks into several isolated segments (with different false colors). (Inset) Ruptured ligaments (purple) in an Au nanomesh chemically bonded on PDMS (green). (C–F) SEM images of prestrained (100%) Au nanomesh on slippery and as-cured substrates during strain cycling. The Au nanomesh on slippery substrate keeps the morphology almost unchanged after 54,000 stretching cycles to 100% (C and D), whereas the Au nanomesh on as-cured substrate forms large cracks (E and F) after only 1,000 stretching cycles to 100%. (Scale bars, 1 μm .) (G) R_s/R_0 and R_t/R_0 as a function of tensile strain for a prestrained (prestrain = 150%) Au nanomesh on slippery PDMS. (H) R_s/R_0 and R_t/R_0 as a function of stretching numbers for prestrained Au nanomeshes immersed in oil. The samples did not show strain fatigue after tens of thousands stretches to a strain of 100, 120, or 150%.

smaller T of 79% and a high R_{sh} of 328 Ω/\square (6). It is worth noting that the decreased adhesion, however, will dramatically deteriorate the scratch resistance so that the Au nanomesh can be wiped off

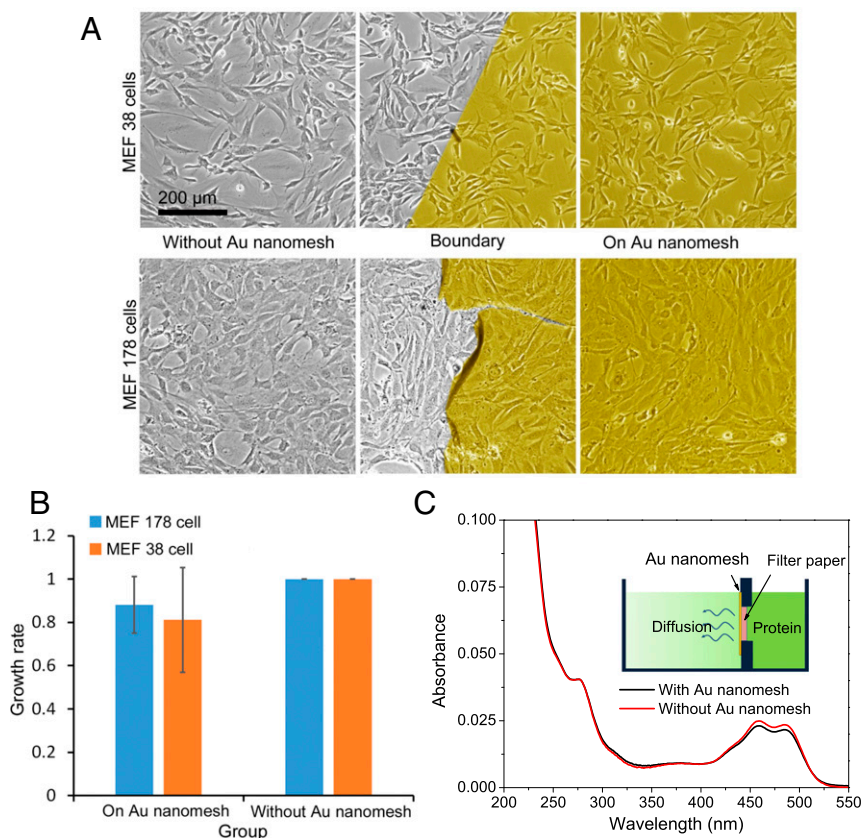


Fig. 4. Biocompatibility and penetrability of Au nanomeshes. (A) Morphology of MEF 38 and MEF 178 cells grown on the Au nanomesh compared with those grown in regular wells. Microscopic images were taken on day 6. The false golden color indicates the Au nanomesh. (Scale bar, 200 μm .) (B) Cell viability assay. MEF cells were seeded at the same density (7×10^3 cells per well) in the 96-well plates covered with and without the Au nanomesh and cultured for 3 d. The related growth rate was evaluated by the CCK-8 reagent. The *P* values of MEF 178 and MEF 38 cells are 0.15 and 0.17, respectively ($n = 4$, Student *t* test). (C) The absorbance spectrum (black line) shows that fluorescent bull serum albumin in solution can pass through the Au nanomesh, and the diffusion rate is close to the case without an Au nanomesh (the spectrum red line).

easily. In this case, the Au nanomesh may be used in applications for which a good adhesion is not required, or be used under protection.

The Biocompatibility and Penetrability of the Au Nanomesh. The large stretchability of Au nanomeshes on a slippery substrate is reminiscent of bioenvironments in which the surface of tissues or organs is slippery or covered by slippery liquid. Thus, the Au nanomesh on tissue or an organ would exhibit large stretchability and accommodate their motion well, without damaging surrounding tissues. Moreover, the Au nanomeshes are biocompatible. In Fig. 4A and B and Fig. S3 we show that MEF cells grow on the Au nanomesh without exhibiting any difference, in either morphology or growth rate, from the cells grown on regular wells for up to 13 d, indicating that the Au nanomesh is nontoxic and is biocompatible. Moreover, the percolating mesh is penetrable to body fluid, allowing biomacromolecules (e.g., protein in Fig. 4C) to pass through freely. This is because the mesh size is far larger than the size of any protein, which is typically only several nanometers (25). Thus, the Au nanomesh might be implanted in the body as a pacemaker electrode, a connection to nerve endings or the central nervous system, a beating heart, and so on.

Conclusions

In summary, we have demonstrated superstretchable and transparent electrodes offering new opportunities for stretchable electronics and transducers. The prestrained Au nanomeshes on slippery substrate demonstrated in this paper can be cyclically stretched to large strains ($>100\%$) for over 50,000 cycles without fatigue. The Au nanomesh electrodes are also expected to be promising for implantable electronics because the nanomeshes mechanically and biochemically match organs or tissues, while causing the least change on the function of both the device and the body.

ACKNOWLEDGMENTS. The work performed at the University of Houston was funded by the US Department of Energy (DOE) under Contract DOE DE-SC0010831/DE-FG02-13ER46917, and that at Harvard University was funded by the National Science Foundation under Materials Research Science and Engineering Center Grant DMR 14-20570. Cell culture performed was supported by National Institutes of Health Grant R01CA155069 (to Z. Shi) and by National Natural Science Foundation of China Grant 81372855. The work was also supported in part by US Air Force Office of Scientific Research Grant FA9550-09-1-0656, the T. L. L. Temple Foundation, the John J. and Rebecca Moores Endowment, and the State of Texas through the Texas Center for Superconductivity at the University of Houston.

- Rowell MW, et al. (2006) Organic solar cells with carbon nanotube network electrodes. *Appl Phys Lett* 88(23):233506.
- Lee JY, Connor ST, Cui Y, Peumans P (2008) Solution-processed metal nanowire mesh transparent electrodes. *Nano Lett* 8(2):689–692.
- Han TH, et al. (2012) Extremely efficient flexible organic light-emitting diodes with modified graphene anode. *Nat Photonics* 6(2):105–110.

- Han B, et al. (2014) Uniform self-forming metallic network as a high-performance transparent conductive electrode. *Adv Mater* 26(6):873–877.
- Zhang D, et al. (2006) Transparent, conductive, and flexible carbon nanotube films and their application in organic light-emitting diodes. *Nano Lett* 6(9):1880–1886.
- Lipomi DJ, et al. (2011) Skin-like pressure and strain sensors based on transparent elastic films of carbon nanotubes. *Nat Nanotechnol* 6(12):788–792.

7. Mineev IR, et al. (2015) Biomaterials. Electronic dura mater for long-term multimodal neural interfaces. *Science* 347(6218):159–163.
8. Liu J, et al. (2015) Syringe-injectable electronics. *Nat Nanotechnol* 10:629–636.
9. Li T, Suo Z, Lacour SP, Wagner S (2005) Compliant thin film patterns of stiff materials as platforms for stretchable electronics. *J Mater Res* 20(12):3274–3277.
10. Lukáš P, Klesnil M, Polak J (1974) High cycle fatigue life of metals. *Mater Sci Eng* 15(2): 239–245.
11. Kim KS, et al. (2009) Large-scale pattern growth of graphene films for stretchable transparent electrodes. *Nature* 457(7230):706–710.
12. Bae S, et al. (2010) Roll-to-roll production of 30-inch graphene films for transparent electrodes. *Nat Nanotechnol* 5(8):574–578.
13. Chen Z, et al. (2011) Three-dimensional flexible and conductive interconnected graphene networks grown by chemical vapour deposition. *Nat Mater* 10(6):424–428.
14. Hu L, Kim HS, Lee JY, Peumans P, Cui Y (2010) Scalable coating and properties of transparent, flexible, silver nanowire electrodes. *ACS Nano* 4(5):2955–2963.
15. Liang J, et al. (2014) Silver nanowire percolation network soldered with graphene oxide at room temperature and its application for fully stretchable polymer light-emitting diodes. *ACS Nano* 8(2):1590–1600.
16. Wu H, et al. (2013) A transparent electrode based on a metal nanotrough network. *Nat Nanotechnol* 8(6):421–425.
17. Liu Y, et al. (2015) A new method for fabricating ultrathin metal films as scratch-resistant flexible transparent electrodes. *J. Materiomics*. 1(1):52–59.
18. Guo CF, Sun T, Liu Q, Suo Z, Ren Z (2014) Highly stretchable and transparent nanomesh electrodes made by grain boundary lithography. *Nat Commun* 5:3121.
19. Hogan B, Beddington R, Costantini F, Lacy E (1994) *Manipulating the Mouse Embryo: A Laboratory Manual* (Cold Spring Harbor Lab Press, Cold Spring Harbor, NY), 2nd Ed.
20. Guo CF, et al. (2013) Conductive black silicon surface made by silver nanonetwork assisted etching. *Small* 9(14):2415–2419.
21. Keplinger C, et al. (2013) Stretchable, transparent, ionic conductors. *Science* 341(6149): 984–987.
22. Guo CF, Lan Y, Sun T, Ren Z (2014) Deformation-induced cold-welding for self-healing of super-durable flexible transparent electrodes. *Nano Energy* 8:110–117.
23. Kim KH, Oh Y, Islam MF (2012) Graphene coating makes carbon nanotube aerogels superelastic and resistant to fatigue. *Nat Nanotechnol* 7(9):562–566.
24. Sim GD, Lee YS, Lee SB, Vlassak JJ (2013) Effects of stretching and cycling on the fatigue behavior of polymer-supported Ag thin films. *Mater Sci Eng A* 575:86–93.
25. Erickson HP (2009) Size and shape of protein molecules at the nanometer level determined by sedimentation, gel filtration, and electron microscopy. *Biol Proced Online* 11(1):32–51.